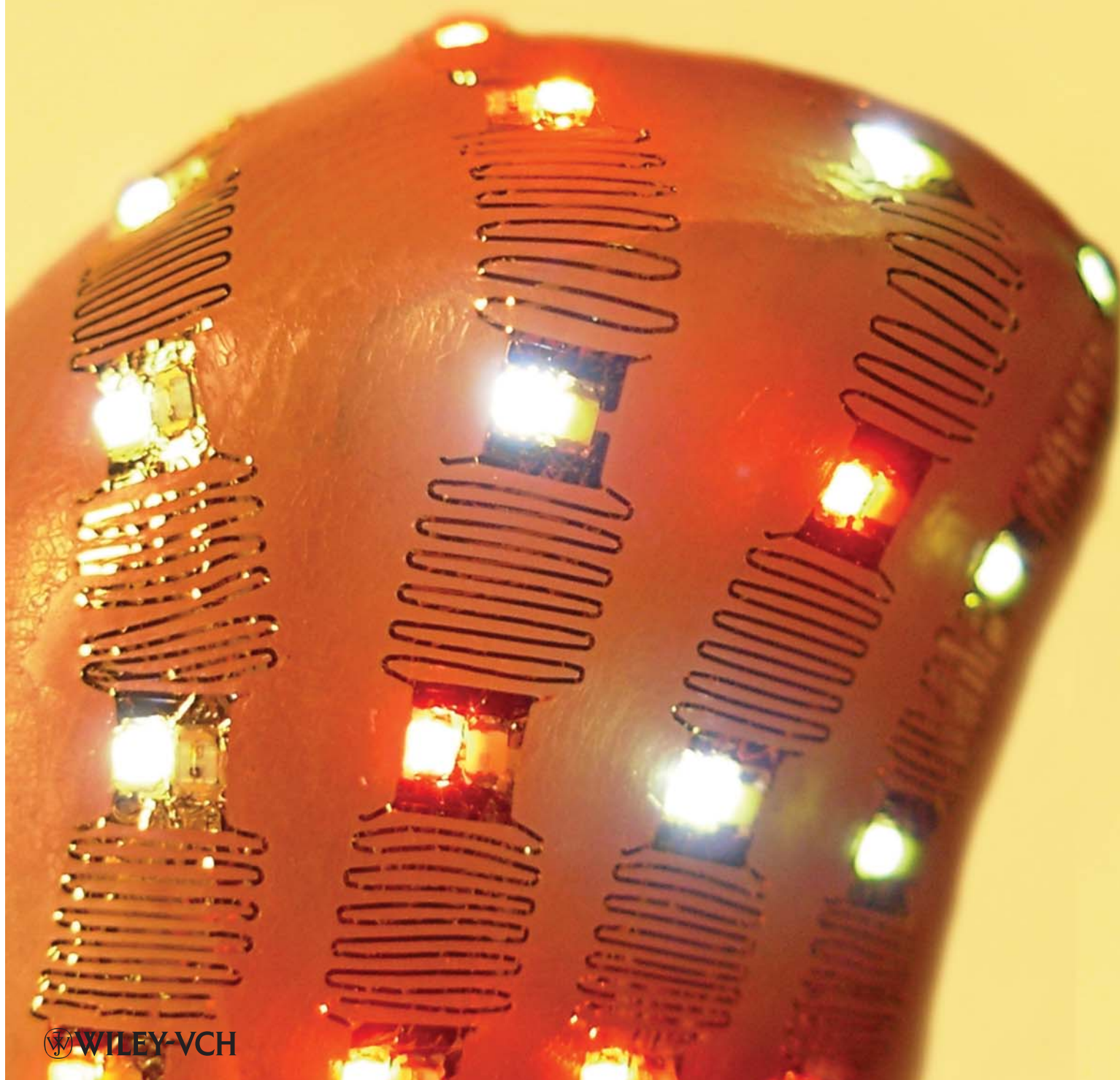


[www.advmat.de](http://www.advmat.de)

# ADVANCED MATERIALS



# Stretchable Inorganic-Semiconductor Electronic Systems

Xiaolong Hu, Peter Krull, Bassel de Graff, Kevin Dowling,\* John A. Rogers, and William J. Arora\*

Electronic and optoelectronic semiconductor components are the building blocks of modern instrumentation and equipment for sensing, computation, display, and communication. Systems incorporating these components are typically made on mechanically rigid printed circuit boards (PCBs). These systems can also be built on polymer-based flexible PCBs,<sup>[1]</sup> which offer a bending radius of several centimeters about a single axis but are subject to fracturing from excessive bending or fatigue strain. Systems that are highly bendable (millimeter scale), stretchable, conformable to any surface topology, and mechanically insensitive to fatigue strain would greatly expand the application space of electronics. For example, in medicine there is a need for electronics to conform to and deform with the human body<sup>[2]</sup> to perform accurate diagnosis and deliver therapy. Other application spaces include renewable energy,<sup>[3,4]</sup> robotics,<sup>[5]</sup> military,<sup>[6]</sup> and lighting.<sup>[7]</sup> These applications have motivated research in flexible and/or stretchable organic electronics<sup>[6,8–9]</sup> and inorganic electronics assembled on stretchable substrates.<sup>[2,4,7,10]</sup> One approach to building stretchable inorganic electronics is to connect thin electronic components together with stretchable spring-like metal interconnects and embed the entire interconnected structure into a stretchable (rubber) substrate.<sup>[2–3,7]</sup> Whereas prior work based on this approach used custom microfabrication of the electronic components and interconnects, here we present a process that uses commercially available electronic components and flip-chip bonding processes. Therefore, this fabrication process is a platform that can be used without modification to create stretchable electronic systems incorporating any set of electronic components. As a demonstration, we fabricated stretchable light-emitting diode (LED) arrays containing up to 50 LEDs and show that the arrays can survive repeated stretching of 90 000 cycles and also tightly conform to a human thumb tip.

The general concept behind the fabrication process is to separately manufacture the electronic components and the stretchable interconnects, then combine them using flip-chip bonding technology. We term this process “CINE” (combination of interconnects and electronics). Specifically, the process involves three steps: 1) the fabrication of metal contact pads and stretchable interconnects using standard microfabrication techniques; 2) transfer printing the contact pads and stretchable interconnects to a stretchable substrate using dissolvable adhesives as the intermediate transfer material; and 3) flip-chip bonding the

electronic components onto the metal contact pads using anisotropic conductive film (ACF). A detailed description of the fabrication process is presented in the Experimental Section.

Figure 1 shows a stretchable LED array fabricated with this process. The stretchable LED array consists of ten pairs of gold contact pads, connected by serpentine-shaped metal interconnects. The interconnects are fully encapsulated in polyimide, whereas the contact pads have openings to allow electrical contact. Five blue and five red LEDs were flip-chip bonded to the pairs of contact pads (in opposing polarities so the array can be powered with either a positive or negative voltage bias). The array was made on a silicone substrate with an elastic modulus of 10 kPa (we used the material EcoFlex made by Smooth-On Inc.). When the array is stretched, the serpentine-shaped interconnects deform to accommodate most of the strain, minimizing the strain seen by the LEDs and allowing the LEDs to maintain their optoelectronic properties (Figure 1c,e). When the substrate is stretched, the interconnects accommodate strain via out-of-plane buckling as well as lateral deformation; this out-of-plane deformation is possible because the EcoFlex substrate is extremely compliant. We measured the resistance of individual interconnects while being stretched and found no significant change in electrical resistance.

To test the mechanical robustness of the arrays, we repeatedly stretched them in the length-wise direction using a mechanical actuator (additional details are provided in the Supporting Information). In the initial state, the array was without any strain, and we measured the distance between two adjacent LEDs as  $L_0$ . When the array was fully stretched, we remeasured the distance between the two adjacent LEDs as  $L_1$ . We define the strain as  $(L_1 - L_0)/L_0$ . With a peak stretching strain of 67%, the arrays survived up to 90 000 stretching cycles (at an oscillating frequency of 1 Hz). With a peak stretching strain of 200%, the arrays survived up to 5000 cycles. We determined the failure mechanism to consistently be fracture–breakage of the serpentine interconnects near the contact pads used for powering the array. These contact pads were too large, at about 1 cm<sup>2</sup> in size, and created regions of high localized strain around their edges. The interconnects connecting adjacent LEDs never failed and neither did the flip-chip bonds made between the LEDs and the contact pads. Therefore, we expect the mechanical robustness of the arrays to dramatically increase simply by redesigning the end-most contact pads to be smaller by a factor of about four.

To examine the electrical robustness, we measured the current–voltage ( $I$ – $V$ ) relation of an LED array prior to being stretched, after being stretched 1000 cycles, and after being stretched 10 000 cycles. We found no significant variation in the  $I$ – $V$  characteristics; the results are presented in Figure 2a. We also measured the current flowing through an array of 15 LEDs (arranged as three parallel sets of five LEDs in-series), biased at 20 V. The current flow was a constant 93 mA as the

Dr. X. Hu, P. Krull, B. de Graff, Dr. K. Dowling, Prof. J. A. Rogers,  
Dr. W. J. Arora  
MC10 Incorporated  
36 Cameron Avenue, Cambridge, MA 02140, USA  
E-mail: kdowling@mc10inc.com; will.arora@alum.mit.edu

DOI: 10.1002/adma.201100144

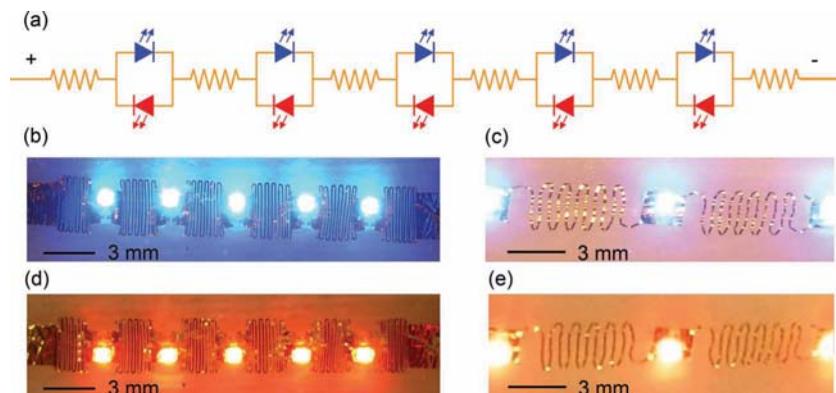


**Figure 1.** A stretchable LED array on an Ecoflex substrate. a) The circuit model for the LED array, consisting of five blue LEDs, five red LEDs, and ohmic interconnects (44  $\Omega$  each). b,d) The array is its unstretched state, biased with + or  $-15$  V. The LED pitch is 3.8 mm and serpentine pitch is 0.5 mm. c,e) The array is stretched 140%. The LED pitch is increased to 9.2 mm, and the serpentine pitch is 1 mm. The amplitude of the serpentine decreased from 3.3 mm to 2.3 mm.

array was repeatedly stretched from 0% strain to 100% strain, indicating no change in electrical resistance of the interconnects or bond pads.

We did, however, observe spectral shifts in the LED optical output during stretching cycles. We measured the spectra by placing the LED array under varying strains next to the input port of a spectrometer. The measurements were taken in a dark room and the background light was measured and subtracted from the spectra measured with the LEDs turned on.

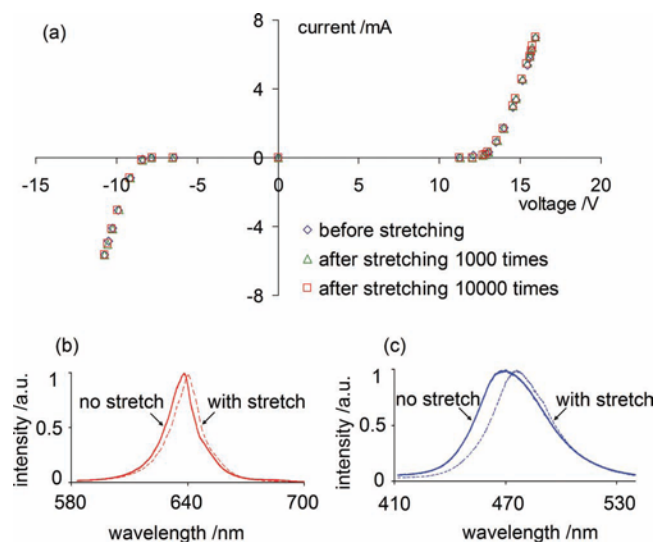


**Figure 2.** Electrical and spectral characterization of the stretchable LED array. a)  $I$ - $V$  relationships were measured before stretching tests, after 1000 stretching cycles, and after 10 000 stretching cycles. The strain in each stretching cycle was 67%, and the  $I$ - $V$  measurements were all taken with 0% strain in the array. Cyclic stretching did not affect the  $I$ - $V$  characteristics of the circuit. b) The spectra of the red LED array measured at 0% strain (solid lines) and 67% tensile strain (dashed lines). The red shift of the spectral peak was 2.3 nm. c) The spectra of the blue LED array measured at 0% strain (solid lines) and 67% tensile strain (dashed lines). The red shift of the spectral peak was 6.8 nm.

We observed red-shifts for both the blue and red LEDs of 6.8 nm and 2.3 nm, respectively, as shown in Figure 2b,c. We hypothesize that the spectral shifts are due to small strains on the semiconductor quantum well induced by stretching the array.

As a more advanced demonstration, we fabricated a stretchable  $5 \times 5$  LED array with each node of the array containing two LEDs, for a total of 50 LEDs. We built three of these arrays and note that we obtained 100% yield of LED bonding in each array. The  $5 \times 5$  array allows for the display of simple alphabetic characters as shown in Figure 3a,b. With the array positively biased, the letter “M” is visible and with the array negatively biased, the letter “C” is visible. In the future, additional switching electronics could be incorporated into each node to create an active display. The LED array can be conformably wrapped onto an arbitrary surface. Figure 3c,d show the

array tightly wrapped around a human thumb. The EcoFlex is about 1-mm thick, and through it the thumb-print and thumb-nail are visible.

The key achievement of this work is not the demonstration of a stretchable inorganic LED array, but the development of the CINE process for making stretchable inorganic semiconductor systems, which is described in detail in the Experimental Section. The commercial LEDs used in this demonstration could be replaced by any other commercial semiconductor components, thereby allowing the creation of any type of stretchable electronic system. Furthermore, the CINE process relies on

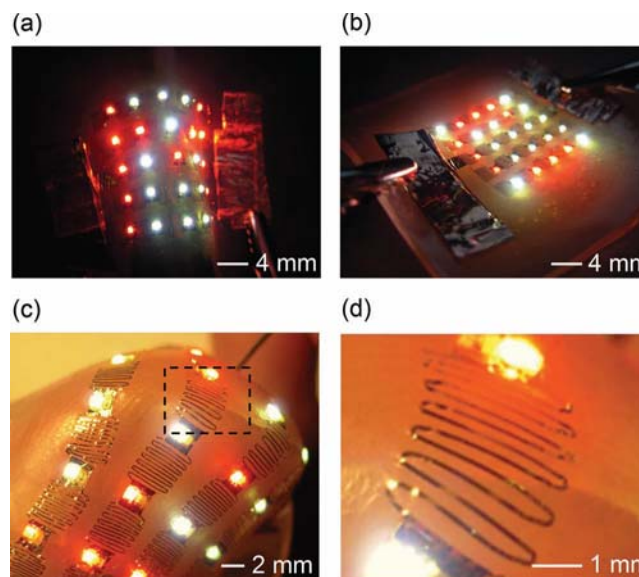


**Figure 3.** A LED array containing 50 LEDs bonded to an Ecoflex substrate, forming a stretchable display panel. a) With the array biased at +15 V, the red LEDs show the letter “M”. b) With the array biased at  $-15$  V, the red LEDs show the letter “C”. c) The LED array tightly wrapped around a human thumb. d) A zoomed-in view of the upper part of the nail, corresponding to the area in the dashed box in (c).

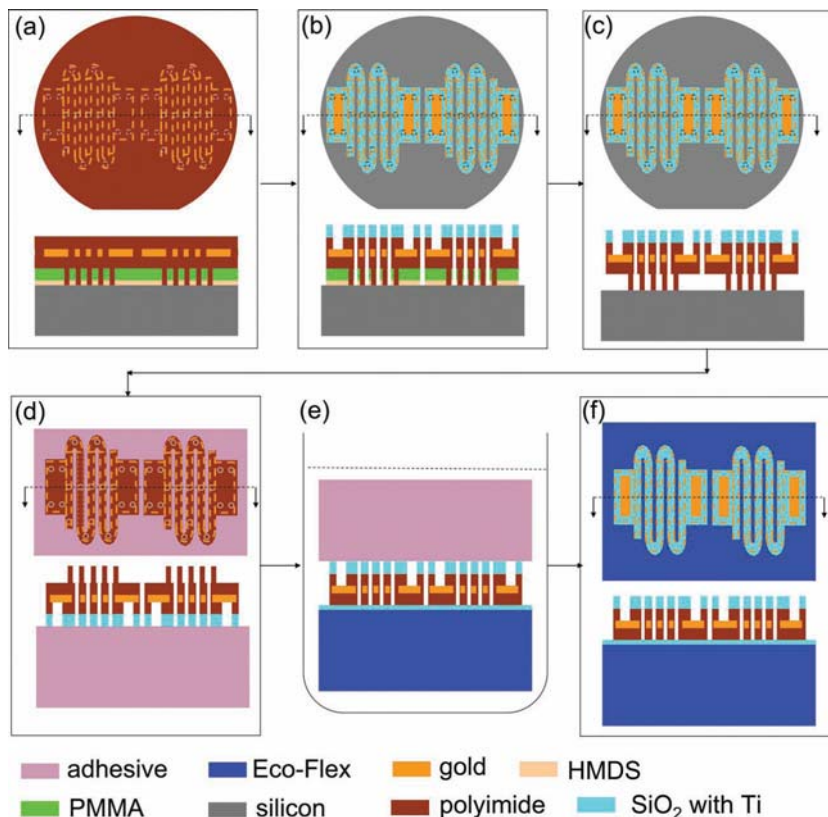


**Figure 4.** Overhead and cross-sectional views of the key fabrication steps, corresponding to the descriptions in the Experimental Section. a) Gold contact pads and interconnects are patterned and encapsulated in polyimide. b) The polyimide is etched around the gold pattern and the electrodes are partially opened to allow contact with electronic components. c) The sacrificial layer is etched in acetone. d) The resulting structure is picked up with an adhesive tape. e) The structure is transferred and bonded to an Ecoflex substrate. Note that the 100-nm-tall polyimide anchor points are not drawn here, as their topology is too small to adversely affect the quality of the bond. f) The adhesive tape is removed leaving the fabricated stretchable interconnect array on Ecoflex.

standard microfabrication processing and is therefore scalable to high-volume, low-cost manufacturing. We believe that the most valuable applications of this technology will be sensor arrays that conform to and deform with the human body, both externally and internally (if the materials used for the sensor arrays are biocompatible), to perform accurate medical diagnostic functions with minimal inconvenience to the patient.

## Experimental Section

**Fabrication:** Gold contact pads and stretchable gold interconnects were fabricated on 4-inch silicon substrates. The surface chemistry of the silicon wafer was modified by priming it with hexamethyldisilazane (HMDS) via spin-coating and baking, ensuring strong adhesion of the subsequent poly(methyl methacrylate) (PMMA) layer to the silicon. Next, a 100-nm-thick layer of PMMA was deposited by spin-coating and baking. 100- $\mu\text{m}$ -diameter holes were etched into the PMMA through a shadow mask using a low-power  $\text{O}_2$  reactive-ion etch (RIE) to minimize spreading of the hole patterns etched through the shadow mask. A 1.5- $\mu\text{m}$ -thick layer of polyimide (PI) was spin-coated and filled in the holes in the PMMA and contacted the silicon substrate through the holes. Later in the sacrificial etch and release step, these locations where the PI contacted the silicon wafer served as anchors to prevent

the interconnect array from floating off of the silicon wafer. The PI was cured at 250 °C for 1 h in an oven. 250 nm of gold was evaporated over the PI, patterned via photolithography (aligned to the holes in the PMMA layer), and wet-etched with the desired contact pad and stretchable interconnect designs. The remaining photoresist was stripped by spinning the wafer and spraying acetone. To encapsulate the gold interconnects and pads, the second 1.5- $\mu\text{m}$ -thick PI layer was spun over the entire wafer and baked at 250 °C for 1 h. **Figure 4a** shows the process at this point. The PI layer was etched into a serpentine structure around the gold pattern. To do this, a 100-nm-thick silicon dioxide ( $\text{SiO}_2$ ) layer was deposited using plasma enhanced chemical vapor deposition (PECVD) as a hardmask. A layer of photoresist was patterned over the  $\text{SiO}_2$  layer aligned to the gold layer and the pattern was transferred through the  $\text{SiO}_2$  layer and through the PI layer with a two-step RIE (tetrafluoromethane ( $\text{CF}_4$ ) chemistry, followed by  $\text{O}_2$  chemistry). The PI was etched down to the silicon (in certain areas, the etch terminated on the gold layer to create exposed electrical contact points), which also removed the photoresist. The remaining  $\text{SiO}_2$  hardmask layer was not stripped. **Figure 4b** shows the process at this point. The sacrificial PMMA layer was dissolved by soaking the wafer in boiling acetone for 2 h. The interconnects did not float away because they were bonded to the silicon wafer by van der Waals forces at the aforementioned anchor point locations. With a diameter of 100  $\mu\text{m}$ , the spacing of these holes was chosen to be 1 mm apart. It is important to limit the total area of the anchor points to prevent too much adhesion force between the polyimide and silicon so that the entire interconnect array can be easily transfer printed off of the wafer in the next step. At the same time, the holes cannot be spaced so far apart to prevent the interconnect array from floating away in the sacrificial etch step. **Figure 4c** shows the process at this point. It is noted that instead of using a shadow mask to pattern the PMMA, one could photoexpose and develop holes in the PMMA using a 220-nm light source and a photomask. This would allow patterning of holes much smaller than 100  $\mu\text{m}$ , but was not necessary for the experiments presented in this paper.

**Transfer Printing:** Next, the interconnect array was covered with tape and pressure was applied by hand to ensure intimate contact between the tape and the array. The tape was peeled off from the silicon substrate by hand, slowly from one end to the other, which removed the entire interconnect array. **Figure 4d** shows the process at this point. 3-nm titanium (Ti) and 30-nm  $\text{SiO}_2$  were evaporated over the backside of the interconnect array (and the sticky side of the tape) to enhance bonding of the array to the Ecoflex in the subsequent step. A 1-mm thick sheet of Ecoflex was prepared as directed by the manufacturer, and then the Ecoflex and the tape were exposed with the array to  $\text{O}_2$  plasma simultaneously, to create highly oxidized surface layers to enhance the subsequent bonding step. The tape was manually contacted and pressed with the array onto the Ecoflex, with 5-kPa pressure for 10 min. As a result, the tape and array covalently bonded to the Ecoflex. **Figure 4e** shows the process at this point. Note that the PI anchor points shown in **Figure 4d** were not removed or flattened; they were only 100 nm in height and their topology was insignificant for the bonding step. They are omitted from the drawing in **Figure 4e** for clarity. The tape was removed and the resistance of each serpentine was measured to be  $44.2 \pm 0.4 \Omega$ . **Figure 4f** shows the process at this point.

**LED Bonding:** LEDs of various colors (Rohm Semiconductor, threshold voltage  $\approx 2$  V, "picoLED" series) with packaged dimensions of 1 mm long, 0.6 mm wide and 0.2 mm thick, having two bottom-side contacts were purchased. Anisotropic conductive film (ACF; 3M) was tacked onto

the entire bottom-side of the LEDs by manually cutting and attaching a piece of ACF onto the LEDs and heating the LEDs at 110 °C on a hotplate with light manual pressure applied with a nonstick surface. A flip-chip bonder (Fineplacer Lambda model made by Finetech) was then used to align and bond the LEDs to the contact pads with a force of 7 N. While applying force, the bottom-plate was heated to 250 °C for 60 s, then cooled to room temperature and the force was removed. Ideally the LEDs would be heated directly from the top but the flip-chip bonder did not allow this. After bonding, the LEDs remained strongly mechanically bonded to the contact pad and were electrically connected as well. The bond resistance was measured to be  $<1 \Omega$ . Previously bonded LEDs were unaffected by the repeated thermal cycling when adding new LEDs. The Ecoflex deformed substantially under the 7-N load but returned to its original form after each bonding procedure. After bonding all of the LEDs in serial fashion, the array was left or a thin layer of Ecoflex was brushed on and cured to provide additional mechanical protection.

## Supporting Information

Supporting Information is available from the Wiley Online Library or from the author.

Received: January 13, 2011

Revised: March 28, 2011

Published online: April, 29 2011

- [1] P. Du, G. O'Grady, J. U. Egbuji, W. J. Lammers, D. Budgett, P. Nielsen, J. A. Windsor, A. J. Pullan, L. K. Cheng, *Ann. Biomed. Eng.* **2009**, 37, 839.
- [2] J. Viventi, D. -H. Kim, J. D. Moss, Y. -S. Kim, J. A. Blanco, N. Annetta, A. Hicks, J. Xiao, Y. Huang, D. J. Callans, J. A. Rogers, B. Litt, *Sci. Transl. Med.* **2010**, 2, 24ra22.
- [3] J. Yoon, A. J. Baca, S.-I. Park, P. Elvikis, J. B. Geddes III, L. Li, R. H. Kim, J. Xiao, S. Wang, T.-H. Kim, M. J. Motala, B. Y. Ahn, E. B. Duoss, J. A. Lewis, R. G. Nuzzo, P. M. Ferreira, Y. Huang, A. Rockett, J. A. Rogers, *Nat. Mater.* **2008**, 7, 907.
- [4] Y. Qi, N. T. Jafferis, K. Lyons Jr., C. M. Lee, H. Ahmad, M. C. McAlpine, *Nano Lett.* **2010**, 10, 524.
- [5] B. Siciliano, K. Oussama, *Handbook of Robotics*, Springer-Verlag, Berlin **2008**, Ch. 19.
- [6] A. D. Francoeur, *Photonics Spectra* **2009**, 43, 50.
- [7] S. -I. Park, Y. Xiong, R.-H. Kim, P. Elvikis, M. Meitl, D.-H. Kim, J. Wu, J. Yoon, C.-J. Yu, Z. Liu, Y. Huang, K.-C. Hwang, P. Ferreira, X. Li, K. Choquette, J. A. Rogers, *Science* **2009**, 325, 977.
- [8] S. R. Forrest, *Nature* **2004**, 428, 911.
- [9] T. Sekitani, U. Zschieschang, H. Klauk, T. Someya, *Nat. Mater.* **2010**, 9, 1015.
- [10] M. Gonzalez, F. Axisa, M. V. Bulcke, D. Brosteaux, B. Vandeveldel, J. Vanfleteren, *Microelectron. Reliab.* **2008**, 48, 825.